Role of Ions in Plasma Polymerization of Cyclopropylamine/Argon Radio Frequency Capatively Coupled Discharges

L. Zajíčková[1,2], M. Michlíček[1,2], Peter Papp[3], Marián Danko[3], Štefan Matějčík[3] and S. Hamaguchi[4]

[1]*RG Plasma Technologies, Central European Institute of Technology, Masaryk University, Brno, Czech Republic*
[2]*Department of Phys. Electronics, Faculty of Science, Masaryk University, Brno, Czech Republic*
[3]*Department of Experimental Physics, Comenius University Bratislava, Slovakia*
[3]*CAMT, Graduate School of Engineering, Osaka University, Japan*

Abstract: Plasma polymers prepared in cyclopropylamine/argon discharges at low pressure were previously reported as platform for successful immobilization of biomolecules, cell adhesion and proliferation. Plasma processes at low pressure can be significantly influenced by positive or negative ions and the film growth can be effected by ions via added mass or energy. Therefore, the ions in CPA/Ar plasma are discussed on the basis of crossed molecular/electron beam single-collision experiments, mass and ion spectrometry of plasma phase and retarding field energy analyzer measurement at the substrate electrode. The influence of Ar^+ bombardment on the growth of cyclopropylamine plasma polymers is assessed using molecular dynamic simulations.

1. Introduction

Thin films containing amine groups are promising for various bio-applications like immunosensors, cell cultivation, tissue engineering and enzyme attachment [1-6]. Plasma enhanced chemical vapor deposition (PECVD) or rather its sub-category, plasma polymerization, is able to produce amine films with varied amount of functionalities and cross-linking degree. Therefore, it is important to understand how the experimental parameters influence the final film. Plasma processes at low pressure can be significantly influenced by positive or negative ions created in the plasma volume. Moreover, the positive ions are accelerated towards substrates through adjacent plasma sheath and contribute to the film growth either by added mass [7] or energy [8]. This paper aims to discuss the creation and effect of ions on the plasma polymerization of cyclopropylamine (CPA) in mixture with Ar. The CPA/Ar mixture was selected among other possible choices [4,8-10] because of previously reported successful bio-related applications of CPA plasma polymers (CPA-PPs) prepared in radio frequency (RF) capacitively coupled plasma (CCP) [5,6] as well as detailed studies of their chemistry [11-12].

2. Plasma polymerization of cyclopropylamine and its diagnostics

Three custom-built vacuum reactors for RF (13.56 MHz) CCP discharges were employed for the deposition of plasma polymers (PPs) from CPA/Ar mixture in continuous wave (duty cycle 100 %) and pulsed (duty cycle 33 %, frequency 500 Hz) modes. The comparison of the films can result in more general conclusions and allow better understanding the influence of energetic conditions at the substrate on the film chemical structure and functional properties CPA-PPs.

In the tubular glass reactor with vertical electrodes, the substrates were placed at the floating potential V_{fl} (Fig. 1). The voltage drop in the plasma sheath could be estimated as [13]

$$V_{fl} = \frac{kT_e}{2e} \ln\left(\frac{2\pi m}{M}\right) \qquad (1)$$

where T_e, m, e are electron temperature, mass and charge, respectively, and M is the mass of ions. Taking into the mass or argon ion the floating potential is $5T_e$, i.e. about 10 V for the estimated electron temperature of 2 eV. The energy of ions accelerated in the sheath adjacent to the floating substrate was decreased even more by the collisions because the deposition took place at 120 Pa.

In the stainless steel reactors with horizontal electrodes the substrates were placed on the bottom RF electrode (Fig. 2). This electrode acquired also DC self-bias due to different areas of grounded and RF surfaces. Therefore, the potential in the plasma sheath can be much higher than in the floating potential case. Previously, the film chemistry and functional properties were discussed for the larger stainless steel reactor with the RF electrode diameter of 420 mm. The top grounded showerhead electrode, 380 mm in diameter, was placed 55 mm from the bottom electrode. The inner diameter of the reactor was 490 mm.
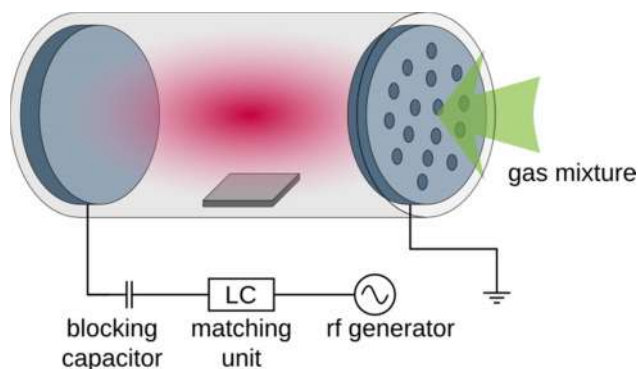

Fig. 1 Scheme of CCP discharge with the substrates at floating potential (at the glass reactor walls)
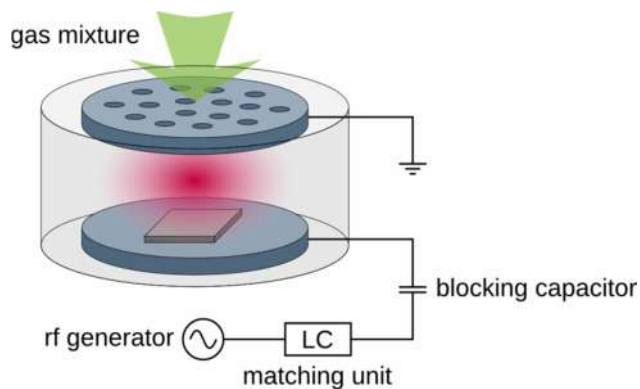
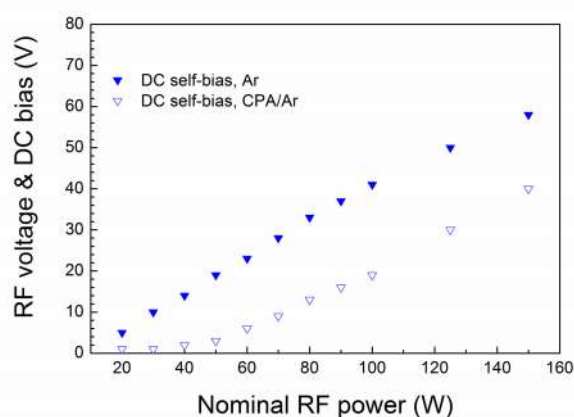Fig. 2 Scheme of CCP discharge with the substrates at the RF electrode.

Fig. 3 RF voltage amplitude and DC self-bias measured in the large stainless steel reactor for the conditions related to the CPA plasma polymerization (p=50 Pa, Q(CPA) = 2sccm, Q(Ar) = 28 sccm) at varied RF power supplied by the generator.

The electrical parameters, delivered RF power, RF voltage amplitude and DC self-bias U_b, were determined by the Octiv VI (Impedans). The dependence of RF voltage and U_b on nominal RF power (delivered by RF generator) are shown in Fig. 3 for the conditions relevant to the carried out depositions, i.e. pressure of 50 Pa, CPA and Ar flow 2 and 28 sccm, respectively. The voltage accelerating ions in the sheath at the RF electrode is the sum of the self-bias U_b and the plasma potential but at the pressure of 50 Pa the collisions decrease the ion energy considerably. Moreover, U_b is close to zero for low RF power because the discharge is not asymmetric, being confined between the electrodes (Fig. 3).

The third CCP reactor had in principle the same configuration as the above described large reactor with horizontal electrodes but it was smaller (inner diameter 250 mm), the RF electrode being 210 mm. The distance between the electrodes was again 55 mm. It was used because of several plasma diagnostics methods available at this reactor (Fig. 4). The ion flux and energy distribution function at the substrate electrode were studied by retarding field energy analyzer (RFEA) at different plasma conditions related to the film deposition. The mass and ion energy spectra of plasma species were acquired with Hiden EQP 500.

The films from all three plasma reactors were compared from the chemical structure point of view using X-ray photoelectron spectroscopy (XPS) carried out with the Axis Supra spectrometer (Kratos Analytical, England) and using infrared spectroscopy with Bruker Vertex 80v spectrometer.
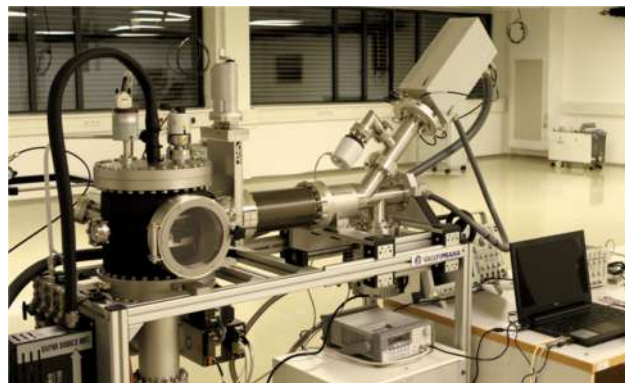

Fig. 4 Photograph of stainless steel CCP reactor with horizontal electrodes (as in scheme in Fig. 2) equipped with plasma diagnostics tool, namely Hiden EQP 500 spectrometer.

3. Crossed electron/CPA molecular beam experiments

The electron ionization and attachment processes were studied with a crossed electron/molecular beams apparatus, schematically depicted in Fig. 5 and described in details elsewhere [14].

The vapors of CPA were introduced into the vacuum through a small capillary 0.5 mm in diameter and 4 mm in length, forming an effusive molecular beam, which was crossed perpendicularly with an electron beam under single-collision conditions. The background pressure was $\sim 10^{-6}$ Pa and the working pressure in the chamber during the measurements was $\sim 10^{-4}$ Pa.

Resistively heated tungsten hairpin filament was used as a source of electrons forming the beam. The electron beam was formed by a trochoidal electron monochromator (TEM) which design is described in [15]. An axial magnetic field ($\sim 10^{-3}$ T) perpendicular to electric field (0-5 V) in a dispersion region of the TEM was used to select the electrons with narrow energy distribution. The energy spread of the electrons in the beam was typically $\sim$ 200 meV FWHM (full width at half maximum). Obtained electron current was typically 80-180 nA. The electron beam was accelerated to desired energy and the collision with a molecular beam occurred in the reaction chamber of TEM. The electron current was measured behind the reaction chamber on a collector plate.

Ions formed in the (dissociative) electron ionization reactions were dragged out of the TEM by weak electric

field into the quadrupole selector of a mass spectrometer. Ions of a selected mass were then analyzed by a channeltron detector.
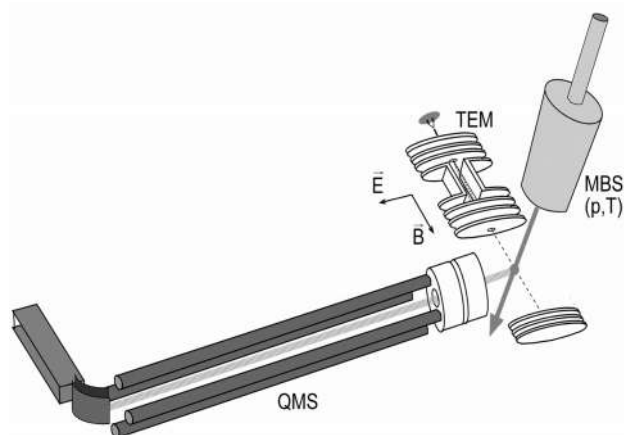

Fig. 5 Schematic drawing of crossed molecular/electron beam apparatus used to investigate appearance energies of CPA fragment ions.

4. Experimental results

Mass spectra of CPA positive ions created by electron impact in crossed beam apparatus at different electron energies were characterized by four groups of ions depending on the number of C plus N atoms in the fragments (from 1 to 4). Similar results were achieved with Hiden spectrometer connected to the PECVD chamber. The example of mass spectra of CPA/Ar mixture used for the deposition of plasma polymers is shown in Fig. 6.

The most dominant ion in all of the spectra above 12 eV is deprotonated CPA (CPA-H)$^+$, mass 56 u, while the second dominant peak is the parent ion CPA$^+$, mass 57 u (C$_3$H$_7$N$^+$). Lower masses in this "C4" group (the most intense being 54 u) occur due to higher deprotonation. The peak at mass 58 u is assigned to CPA isotope.

In case of CPA/Ar mixture the group "C3" contains also intense Ar$^+$ peak at 40 and other two less abundant isotopes (36, 38). Besides, the peaks originating from the dissociation of CPA appear at 39, 41, 42 and 43 u. Dennis et al. [16] did not reported them for the electron ionization energy of 20 eV but the highly sensitive measurements in crossed beams apparatus at 20 eV and also Hiden spectrometer measurements at 25 eV reveal their presence. These peaks have ambiguous assignments referring to either three C atoms or two C atoms and one N, e.g. C$_3$H$_3$ or C$_2$HN for 39 u.

At 10 eV, only two ions remain besides 56 and 57 u. One is NH$_3^+$ (mass 17 u), which is important for the plasma polymerization processes leading to formation of amine-rich thin films. The other is CH$_4$N$^+$/C$_2$H$_6^+$ (mass 30 u). According to our *ab-initio* calculations the formation of CH$_4$N$^+$ is more probable.
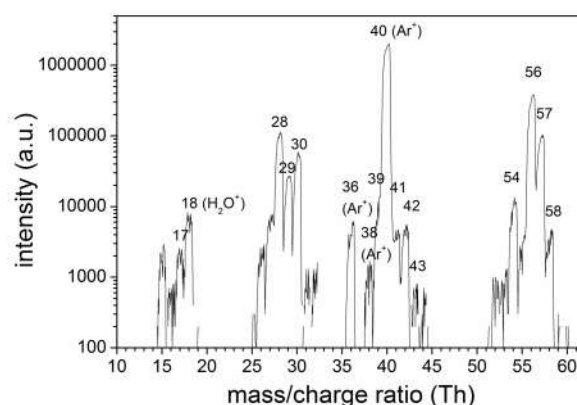

Fig. 6 Mass spectra of CPA/Ar gas mixture.

Mass spectrometry of CPA/Ar plasma phase revealed numerous fragments created in the discharge, most of which are rapidly consumed when the discharge power is increased. Notable exceptions are fragments at 27 and 28 u which are rapidly produced from original CPA molecule and probably have a relatively low sticking coefficient. In the ion mass spectra, surprisingly large populations of heavy ions were found under conditions with lower specific power. This suggests high importance of ionic nucleation reactions in the gas phase which are at higher specific power suppressed by competitive process of electron impact dissociation.

In CPA/Ar discharges, especially at higher RF power, the formation of dust particles was observed because the white powder was collected at the edges of the RF electrode surrounded by a grounded ring. The formation of dust particles in plasmas in usually attributed to the presence of negative ions that are abundantly formed e.g. in acetylene discharges [17]. However, we note that negative ions could not be detected in the experimental set up studying the electron attachment processes for CPA. Therefore, it is assumed that the negative ions are formed by electron attachment to CPA fragmentation products rather than by direct electron attachment to CPA.

Using RFEA, we confirmed our hypothesis that ion bombardment and corresponding energy flux towards the growing surface is significant even at high pressure when plasma sheath is dominated by collisions. This result can be applied for comparison of other reactors used for Ar/CPA deposition which have different sheath potentials. It should be also noted that ion energies and fluxes are quite different between discharges in pure Ar and Ar/CPA mixture. Therefore, models of collisional sheaths developed for pure Ar cannot be directly used to estimate ion energy and flux.

5. MD simulations

Using classical molecular dynamics (MD) simulations the process mimicking the plasma polymerization from CPA/Ar mixture on polystyrene surface, used conventionally for cell cultivation studies, was studied in

a simplified manner considering only CPA molecules and Ar ions. Abundant low energy CPA molecules (4x16 units, energy of 0.1 eV) were injected in the simulations alternatively with energetic Ar ions (1 unit, energy up to 100 eV). The scheme of this in-silico experiment is in Fig. 7.

The simulation code worked with modified interatomic potential functions of Stillinger-Weber type, whose parameters were determined from *ab initio* simulations of small atomic clusters. Periodic x-y boundary conditions were considered. In each injection of an ion or a neutral species, the simulation with constant total energy (i.e., microcanonical simulation) was carried out for 1.7 picoseconds and then the system was cooled down to the room temperature for the subsequent 0.3 picoseconds. The simulation cycle was repeated 1000 times. Example of the results at the end of the simulation for Ar^+ energy of 100 eV is in Fig. 8.

Results of the MD simulations under the conditions simplifying the process of plasma polymerization from CPA/Ar mixture indicate that most amines formed in these processes are secondary amines.
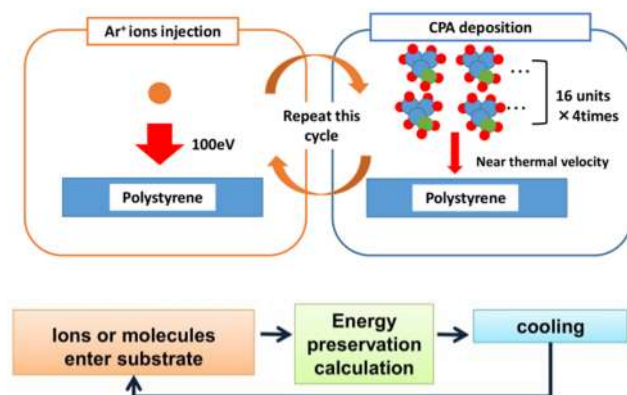
Fig. 7 Scheme of the MD simulation cycle mimicking the deposition of films from CPA/Ar CCP discharge.
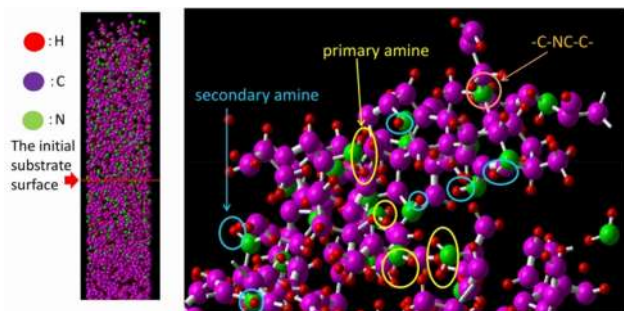
Fig. 8 Result of MD simulation according to the scheme in Fig. 7 (Ar^+ energy 100 eV).

References
[1] K. Siow, L. Britcher, S. Kumar, H. Grieser, Plasma Process. Polym. **3**, 392 (2006).
[2] H. Biederman, I. Boyaci, P. Bilkova, D. Slavinska, S. Mutlu, J. Zemek, M. Trchova, J. Klimovic, M. Mutlu, J. Appl. Polym. Sci. **81**, 1341 (2001).
[3] R. Nakamura, H. Muguruma, K. Ikebukuro, S. Sasaki, R. Nagata, I. Karube, H. Pedersen, Anal. Chem. **69**, 4649 (1997).
[4] D. E. Robinson, S. A. Al-Bataineh, B. L. Farrugia, A. Michelmore, A. J. Cowin, T. R. Dargaville, R. D. Short, L. E. Smith, J. D. Whittle, Plasma Process. Polym. **13**, 678 (2016).
[5] E. Makhneva, Z. Farka, P. Skádal, L. Zajíčková, Sensors & Actuators: B. Chemical **276**, 447 (2018).
[6] A. Manakhov, E. Kedroňová, J. Medalová, P. Černochová, A. Obrusník, M. Michlíček, D. Shtansky, L. Zajíčková, Materials & Design **132**, 257 (2017).
[7] A. Michelmore, J. D. Whittle, R. D. Short, Frontiers in Physics: Plasma Physics **3**, Article 3 (2015).
[8] D. Hegemann, E. Körner, N. Blanchard, M. Drabik, S. Guimond, Appl. Phys. Lett. **101**, 211603 (2012).
[9] M. Buddhadasa, P.-L. Girard-Lauriault, Thin Solid Films **591**(A), 76 (2015).
[10] M. Müller, C. Oehr, Surf. Coat. Technol. **116–119**, 802 (1999).
[11] A. Manakhov, L. Zajíčková, M. Eliáš, J. Čechal, J. Polčák, J. Hnilica, Š. Bittnerová, D. Nečas, Plasma Process. Polym. 11, 532 (2014).
[12] A. Manakhov, M. Landová, J. Medalová, M. Michlíček, J. Polčák, D. Nečas, L. Zajíčková, Plasma Process. Polym. 14, e1600123 (2017).
[13] M. A. Lieberman, A. J. Lichtenberg, Principles of Plasma Discharges and Materials Processing, Wiley 2005.
[14] M. Stano, Š. Matejčík, J.D. Skalný, T D Märk: Journal of Physics B **36**, 261 (2003).
[15] J. Matúška, D. Kubala, Š. Matejčík: Measurement Science and Technology **20**, 015901 (2009).
[16] L. Denis, P. Marsal, Y. Olivier, T. Godfroid, R. Lazzaroni, M. Hecq, J. Cornil, R. Snyders, Plasma Process. Polym. **7** (2), 172 (2010).
[17] Ch. Deschenaux, A. Affolter, D. Magni, C. Hollenstein, P. Fayet, J. Phys. D: Appl. Phys. **32**, 1876 (1999).